

Na<sup>+</sup> Specific Emission Changes in an Ionophoric Conjugated PolymerKhushrav B. Crawford,<sup>‡</sup> Marc B. Goldfinger,<sup>†</sup> and Timothy M. Swager<sup>\*‡</sup>

Contribution from the Departments of Chemistry, Massachusetts Institute of Technology, 77 Massachusetts Avenue, Cambridge, Massachusetts 02139, and University of Pennsylvania, Philadelphia, Pennsylvania 19104

Received October 27, 1997

**Abstract:** The emission and absorption characteristics of a conjugated poly(phenylene bithiophene), **2**, and a monomeric model compound, **3**, were investigated as a function of [Li<sup>+</sup>], [Na<sup>+</sup>], [K<sup>+</sup>], and [Ca<sup>2+</sup>]. The calix-[4]arene bithiophene receptor that is present in both **2** and **3** provides selectively for Na<sup>+</sup> and the absorption and emission characteristics are not affected by Li<sup>+</sup>, K<sup>+</sup>, or Ca<sup>2+</sup>. Both systems display absorption spectra which are relatively insensitive to Na<sup>+</sup>; however, the Stokes shift of the emission is reduced by added Na<sup>+</sup>. For the model system **3**, increasing [Na<sup>+</sup>] provides a shift of the emission that is consistent with an equilibrium mixture of bound and unbound receptor. The polymer **2** displays a larger shift in the emission in response to Na<sup>+</sup> and due to multiple binding sites lacks an isoemissive point. The chain length of the polymer also has an effect on this behavior. This behavior may be due to energy migration to regions of the polymer which do not have bound Na<sup>+</sup> and can relax to lower energy conformations. This description is also borne out by the reduction in the lifetimes of the excited states with increasing [Na<sup>+</sup>] for both the polymer **2** and the model system **3**. This mechanism may provide a route to systems which can function as digital indicators at critical concentrations of analytes.

## Introduction

The construction of a useful molecule-based sensory material is dependent on two general design features.<sup>1</sup> One requirement is that a reversible recognition element be present to provide selectivity for a given analyte. The second general requirement is that the molecule-based sensor must be able to exhibit a measurable response, such as a change in color, emission, redox potential, or conductivity, in response to the recognition event. The development of recognition sites has been vigorously pursued in recent years, and an enormous literature describing synthetic receptors has developed.<sup>2</sup> There has also been considerable effort directed toward the design and development of chemosensors for metal ions.<sup>3</sup> Recently Wasielewski and Wang reported some novel conjugated polymer systems that can be used as sensors for transition metals.<sup>4</sup> In this report we describe the fluorescent sensory behavior of a poly(phenylene

bithiophene) that contains a calixarene-based ion receptor, as well as its monomeric molecular analogue. These materials display exceptional selectivity for the Na<sup>+</sup> ion, as no chemosensory response was observed on exposure to Li<sup>+</sup>, K<sup>+</sup>, or Ca<sup>2+</sup> ions. On the basis of our previous investigations of conjugated polymer-based fluorescence,<sup>5</sup> we believe that energy migration may play a role in defining the emission characteristics. In the present study we provide evidence that energy migration processes can result in a different behavior wherein the emission is less affected below a critical concentration of analyte, whereas above this concentration the system switches to a different emission wavelength. Further development of systems displaying this behavior can provide an approach to sensors displaying a threshold or digital response.

## Results and Discussion

As detailed in Scheme 1 copolymerization of a calixarene-based bithiophene receptor, **1**,<sup>6</sup> with a bifunctional phenylene unit, produces conjugated polymer **2**. Model system **3** was similarly prepared to aid in identifying the photophysical phenomena that arise from the special characteristics of the polymer system. Polymer **2** is obtained as a yellow-orange solid with  $M_n = 4500$  g/mol and PDI = 1.55 (GPC vs polystyrene standards, THF eluent) and is very soluble in common organic solvents such as CHCl<sub>3</sub>, CH<sub>2</sub>Cl<sub>2</sub>, and THF.

The measurements of both **2** and **3** reported in Figures 1 and 2 were performed at a concentration of  $5.0 \times 10^{-6}$  M in THF. The concentration of **2** is based on the moles of the repeat unit. The plot of emission intensity at a single wavelength for both

<sup>†</sup> Part of this work was taken from the thesis of MBG completed at the University of Pennsylvania. Present Address: DuPont Central Research and Development, Experimental Station, Wilmington, DE 19880.

<sup>‡</sup> Present address: Department of Chemistry, Massachusetts Institute of Technology, Cambridge, MA 02139.

(1) Brzózka, Z. (Chapter 8); Osa, T., Anzai, J.-I. (Chapter 9); Pietraszkiewicz, M. (Chapter 10) In *Comprehensive Supramolecular Chemistry*; Reinhoudt, D. N., Vol. 10, Ed.; Atwood, J. L., Davies, J. E. D., Macnicol, D. D., Vögtle, F., Lehn, J.-M., Eds.; Pergamon: New York, 1996.

(2) (a) Vögtle, F. *Supramolecular Chemistry*; Wiley: New York, 1991. (b) *Fluorescent Chemosensors for Ion and Molecular Recognition*; Czarnik, A. W., Ed.; ACS Symp. Ser. No. 538; American Chemical Society: Washington, DC, 1993. (c) Reinhoudt, D. N. *Recl. Trav. Chim.* **1996**, *115*, 109.

(3) (a) Bissell, R. A.; de Silva, P.; Gunaratne, H. Q. N.; Lynch, P. L. M.; Maguire G. E. M.; McCoy, C. P.; Sandanayake, K. R. A. S. *Top. Curr. Chem.* **1993**, *168*, 223. (b) Valeur, B. Principles of fluorescent probe design for ion recognition. In *Topics in Fluorescence Spectroscopy, Vol. 4: Probe design and chemical sensing*; Lakowicz, J. R., Ed.; Plenum Press: New York, 1994; 21–48. (c) Swager, T. M.; Marsella, M. J. *J. Adv. Mater.* **1994**, *6*, 595. (d) da Silva, A. P.; Gunaratne, H. Q. N.; Gunnlaugsson, T.; Huxley, A. J. M.; McCoy, C. P.; Rademacher, J. T.; Rice, T. E. *Chem. Rev.* **1997**, *97*, 1515.

(4) Wang, B.; Wasielewski, M. R. *J. Am. Chem. Soc.* **1997**, *119*, 12.

(5) (a) Zhou, Q.; Swager, T. M. *J. Am. Chem. Soc.* **1995**, *117*, 12593–12602. (b) Zhou, Q.; Swager, T. M. *J. Am. Chem. Soc.* **1995**, *117*, 7017–8. (c) Goldfinger, M. B.; Swager, T. M. *J. Am. Chem. Soc.* **1994**, *116*, 7895–6.

(6) Marsella, M. J.; Newland, R. J.; Carroll, P. J.; Swager, T. M. *J. Am. Chem. Soc.* **1995**, *117*, 9842–9848.

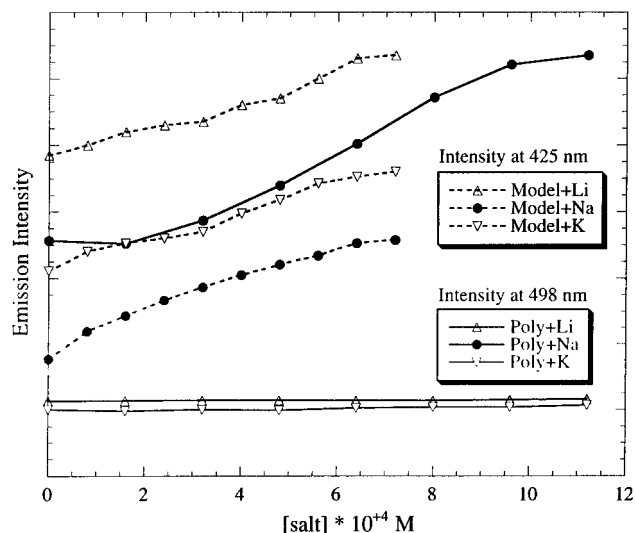
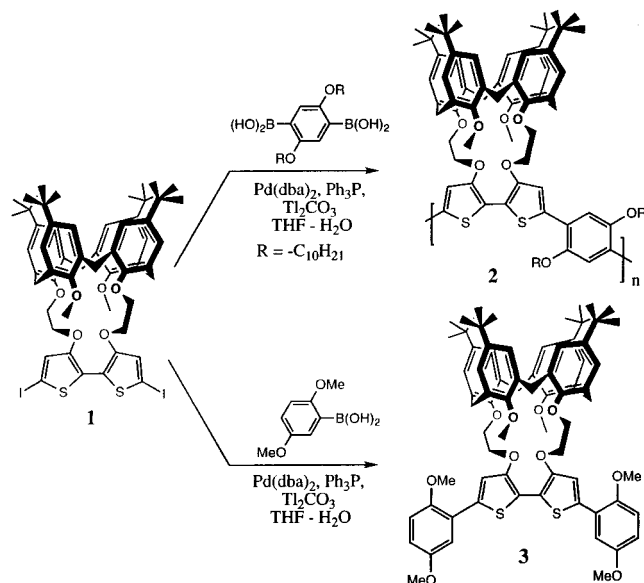


**Figure 1.** Fluorescence intensity for **2** (at 498 nm) and **3** (at 425 nm) as a function of added  $\text{Li}^+$  (open triangle),  $\text{Na}^+$  (closed circle), and  $\text{K}^+$  (open inverted triangle). The solid lines are for polymer **2** and the dashed lines are for model **3**.

### Scheme 1



the polymer **2** and the model **3** as a function of added salt is shown in Figure 1. For the polymer **2** we have chosen to observe the fluorescence intensity at 498 nm since that is the  $\lambda_{\text{max}}$  of the new band growing in due to the addition of  $\text{Na}^+$ . Should one wish to use **2** as a  $\text{Na}^+$  sensor in a detection system, it is best to observe its fluorescence at 498 nm where the  $\text{Na}^+$ -induced changes are the most significant. We have plotted the fluorescence intensity at 425 nm for **3**. Addition of  $\text{Li}^+$  or  $\text{K}^+$  had no effect on the emission of **2** ( $\lambda_{\text{max}} = 548 \text{ nm}$ ) other than to reduce the fluorescence intensity slightly. This is manifested in the near independence of fluorescence intensity as a function of  $[\text{Li}^+]$  or  $[\text{K}^+]$ . In the case of both  $\text{Li}^+$  and  $\text{K}^+$  ions no change is observed in the UV-vis spectra for either polymer **2** or model **3**.

The absorption and emission spectra of **2** and **3** as a function of  $[\text{Na}^+]$  are shown in Figure 2. Compound **3** ( $\Phi_{\text{F}} = 0.029$ ) shows a slight change in its UV-vis spectrum upon addition of  $\text{Na}^+$ , with a  $[\text{Na}^+]$ -independent  $\lambda_{\text{max}}$  and the onset of absorption a very slight blue shift with increasing  $[\text{Na}^+]$ . Both of these changes take place nearly linearly with respect to salt

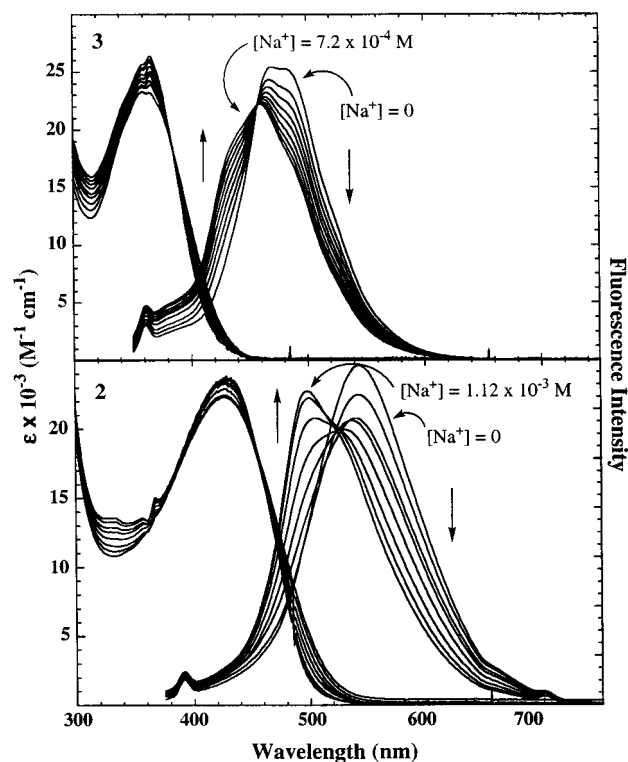


**Figure 2.** Absorption and emission spectra of **2** (bottom) and **3** (top) as a function of increasing  $[\text{Na}^+]$ . For **2**  $[\text{Na}^+]$  increased from 0 M to  $1.12 \times 10^{-3} \text{ M}$  in increments of  $1.6 \times 10^{-4} \text{ M}$ . For **3**  $[\text{Na}^+]$  increased from 0 M to  $7.2 \times 10^{-4} \text{ M}$  in increments of  $8.0 \times 10^{-5} \text{ M}$ . Excitation wavelength was 350 nm for **2** and 320 nm for **3**.

concentration. Compound **3** shows a 26 nm blue shift in its wavelength of emission (from  $\lambda_{\text{max}} = 484 \text{ nm}$  ( $[\text{Na}^+] = 0 \text{ M}$ ) to  $\lambda_{\text{max}} = 458 \text{ nm}$  ( $[\text{Na}^+] = 7.2 \times 10^{-4} \text{ M}$ ) on treatment with  $\text{NaClO}_4$  in increments of  $8.0 \times 10^{-5} \text{ M}$ .

The most dramatic results are observed for the polymer system **2** ( $\Phi_{\text{F}} = 0.16$ ) on treatment with  $\text{Na}^+$  ion (added as  $\text{NaClO}_4$ ) in increments of  $1.60 \times 10^{-4} \text{ M}$  (see Figure 2). The change in the emission is large (from  $\lambda_{\text{max}} = 548 \text{ nm}$  ( $[\text{Na}^+] = 0 \text{ M}$ ) to  $\lambda_{\text{max}} = 498 \text{ nm}$  ( $[\text{Na}^+] = 1.12 \times 10^{-3} \text{ M}$ )). Initial addition of  $\text{Na}^+$  ion produces essentially no response until a critical  $\text{Na}^+$  ion concentration is reached when the wavelength of emission shifts very rapidly from 548 to 498 nm. The UV-vis spectrum is significantly less responsive; however, a similar response can be observed as the absorption remains essentially identical until the critical  $\text{Na}^+$  ion concentration is reached, at which point a very small increase in the absorbance at  $\lambda_{\text{max}}$  is observed. Similar to **3** this is accompanied by a slight blue shift for **2**'s onset of absorption but no shift in the  $\lambda_{\text{max}}$ .

From Figure 2, it is clear that in the case of **3**, there is a clean isosbestic point in the UV-vis and an equally clean isoemissive point in the emission. This appears to imply that **3** forms a 1:1 complex with  $\text{Na}^+$ .<sup>7</sup> Applying the method of Benesi and Hildebrand to the UV-vis and emission data shown in Figure 2, we calculated the binding constant of  $\text{Na}^+$  with **3** to be  $1.9 \times 10^3 \text{ M}^{-1}$ .<sup>8</sup>

Given the high  $\text{Na}^+$  sensitivity of **2** and **3** we also investigated  $\text{Ca}^{2+}$ , which has the same size as  $\text{Na}^+$ . Treatment of THF solutions of **2** and **3** with  $\text{Ca}(\text{ClO}_4)_2$  showed no effect on either the UV-vis or the emission spectra of **2** or **3** even when used in greater than 100-fold excess. The enthalpy of solvation is

(7) Connors, K. A. In *Binding Constants: The Measurement of Molecular Complex Stability*; Wiley-Interscience, New York, 1987, pp 141–155.

(8) Benesi, H.; Hildebrand, J. H. *J. Am. Chem. Soc.* **1949**, *71*, 2703.

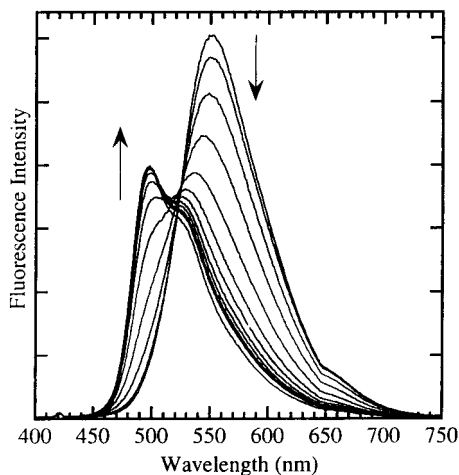


**Figure 3.** Emission curves for **2-H** as a function of added Na<sup>+</sup>. [Na<sup>+</sup>] increases from 0 M to 2 × 10<sup>-3</sup> M in increments of 2 × 10<sup>-4</sup> M. Excitation wavelength = 375 nm.

greater for Ca<sup>2+</sup> than for Na<sup>+</sup>.<sup>9</sup> Also Na<sup>+</sup> prefers to be six coordinate whereas Ca<sup>2+</sup> prefers to be eight coordinate.<sup>10</sup> An interplay of these two factors may be responsible for the insensitivity of **2** and **3** to Ca<sup>2+</sup>.

To gain a deeper insight we determined the emission lifetimes of the various species involved. These measurements were carried out with the model compound **3** and the polymer **2**; first in the absence of Na<sup>+</sup>, then in the presence of an intermediate amount of Na<sup>+</sup>, and finally in the presence of excess Na<sup>+</sup>. The lifetimes were determined by the phase-modulation method over a broad frequency range at a concentration of 2.4 × 10<sup>-5</sup> M.

Polymer **2** exhibited a complex multiexponential behavior that could not be satisfactorily deconvoluted. To obtain a qualitative picture, the decay was approximated to a single exponential. In the absence of Na<sup>+</sup> the lifetime was found to be 0.40 ns, which decreased very slightly to 0.38 ns in the presence of 4 × 10<sup>-4</sup> M Na<sup>+</sup> and then to 0.25 ns when the [Na<sup>+</sup>] increases to 1.2 × 10<sup>-3</sup> M.

With the addition of Na<sup>+</sup>, we expected **3** to be a two-state system (vide infra) and display double exponential decay. However, the lifetimes were of a similar magnitude and were short relative to the time resolution of our instrument (0.01 ns), thereby preventing deconvolution of the two emitting species. Thus **3**'s lifetime was also fit to a single-exponential decay. In the absence of Na<sup>+</sup>, **3** shows a lifetime of 0.15 ns, which decreases slightly to 0.13 ns in the presence of 4 × 10<sup>-4</sup> M Na<sup>+</sup> and then to 0.10 ns when the [Na<sup>+</sup>] increases to 1.2 × 10<sup>-3</sup> M.

In view of the significant difference in the behavior of the model **3** and polymer **2**, we decided to study the effect of chain length. The polymer **2** was fractionated by gel permeation chromatography (THF as the eluent) into three fractions: a high fraction **2-H** ( $M_n = 9600$ , PDI = 1.17, degree of polymerization ~7), a middle fraction **2-M** ( $M_n = 4800$ , PDI = 1.31, degree of polymerization ~4), and a low fraction **2-L** ( $M_n = 2500$ , PDI = 1.31, degree of polymerization ~2).

Measurements for **2-H**, **2-M**, and **2-L** were performed at 2.4 × 10<sup>-5</sup> M (based on repeat unit molecular weight) in THF. The [Na<sup>+</sup>] was changed in steps of 2 × 10<sup>-4</sup> M from 0 M to a maximum of 2 × 10<sup>-3</sup> M. As shown in Figures 3 and 4,

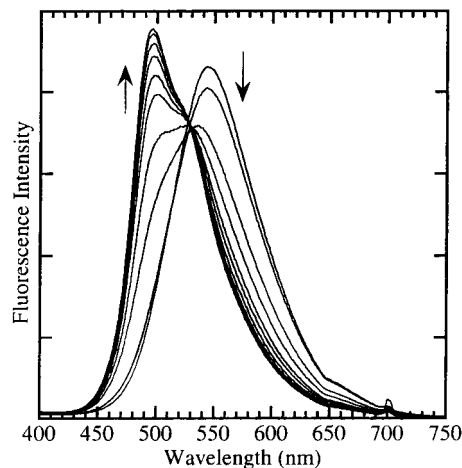


**Figure 4.** Emission curves for **2-M** as a function of added Na<sup>+</sup>. [Na<sup>+</sup>] increases from 0 M to 2 × 10<sup>-3</sup> M in increments of 2 × 10<sup>-4</sup> M. Excitation wavelength = 350 nm.

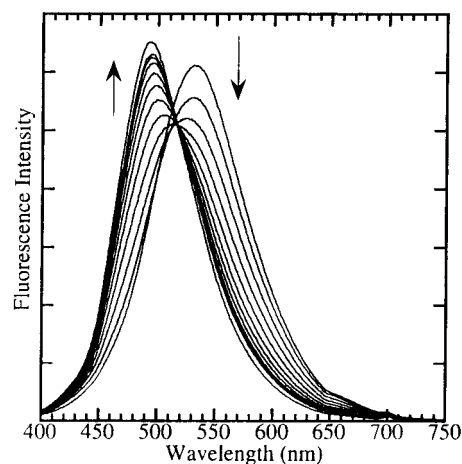


**Figure 5.** Emission curves for **2-L** as a function of added Na<sup>+</sup>. [Na<sup>+</sup>] increases from 0 M to 2 × 10<sup>-3</sup> M in increments of 2 × 10<sup>-4</sup> M. Excitation wavelength = 350 nm.

treatment of **2-H** and **2-M** with Na<sup>+</sup> gave results which are roughly similar to those obtained for the unfractionated polymer **2**. Treatment of **2-L** with Na<sup>+</sup> gives different results as shown in Figure 5. In the absence of Na<sup>+</sup> **2-L** has an emission maximum of 533 nm, which in the presence of Na<sup>+</sup> shifts to 493 nm. In this case the shift is not as abrupt as is the case for **2** and **2-H**, nor is it as gradual as in the case of **3**. In the case of **2-H**, **2-M**, and **2** the emission spectra in the presence of greater than critical [Na<sup>+</sup>] show a shoulder on the low energy side of  $\lambda_{max}$  (at around 520 nm). This shoulder is absent in the case of **2-L**. It is also interesting that this shoulder is less pronounced in the case of **2-M** as compared to **2-H**. As is observed for **2**, the UV-vis spectra for **2-H**, **2-M**, and **2-L** are essentially unchanged upon addition of Na<sup>+</sup>. At this juncture it is worth pointing out that although initially no Na<sup>+</sup> was added, it is quite likely that all samples contained at least a small amount of Na<sup>+</sup>, which is after all a ubiquitous contaminant from silica gel chromatography (employed for purification of monomers and their precursors) and glass containers.

Consideration of this behavior allows us to describe the physical events which are occurring and giving rise to the observed phenomena (see Figure 6). We know from X-ray crystallographic analysis that the thiophene-thiophene bond of the calixarene bithiophene monomer (**1** without the iodides) displays a dihedral angle of 68°.<sup>6</sup> Complexation with the Na<sup>+</sup>

(9) Gokel, G. *Crown Ethers and Cryptands*, 2nd ed.; The Royal Society of Chemistry: Cambridge, 1994.

(10) Greenwood, N. N.; Earnshaw, A. *Chemistry of the Elements*, 1st ed.; Pergamon Press: New York, 1994.

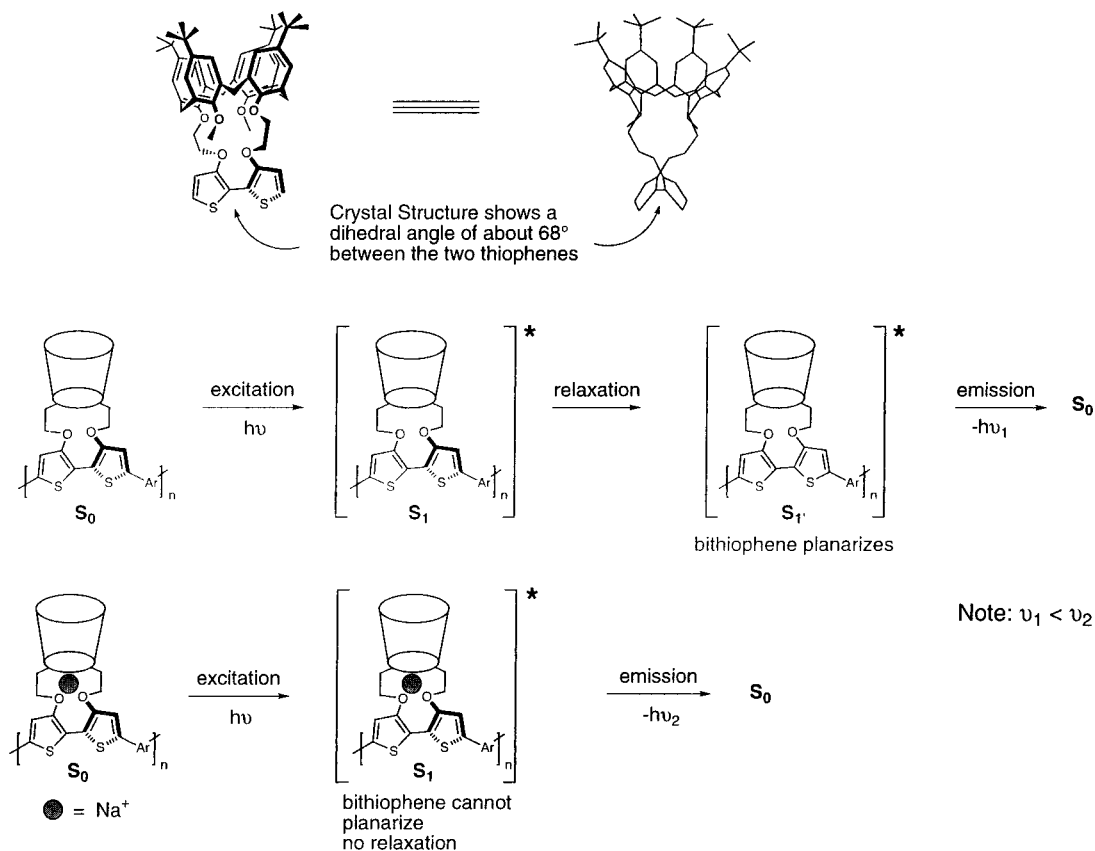


**Figure 6.** 3-D representation of the calixarene-bithiophene subunit (top). Schematic representation of the proposed explanation of the blue shift due to added  $\text{Na}^+$  (bottom). In the absence of  $\text{Na}^+$ , the bithiophenes planarize in the excited state and thus emit at a longer wavelength. In the  $\text{Na}^+$  bound species, this planarization is not possible, shifting the emission to a shorter wavelength.

ion has the potential to either create a greater twist in the bithiophene or perhaps lower the dihedral angle, bringing the thiophene rings into greater conjugation. On the basis of the very low sensitivity of the absorption spectra of both **2** and **3** to the addition of all ions, including  $\text{Na}^+$ , it is apparent that complexation does not induce a significant twist in the bithiophene subunit. The observation that the absorption spectra of both **2** and **3** remain essentially unaltered, while the emission wavelength changes with increasing  $\text{Na}^+$  ion concentration, suggests that in the absence of  $\text{Na}^+$  the first excited-state  $S_1$  undergoes a reorganization to a lower energy state  $S_1'$  before radiative decay occurs. In the case where the calixarenes are complexed with  $\text{Na}^+$  ions, the system is conformationally locked, not allowing reorganization of the excited state, and giving rise to an emission band at higher energy. In other words,  $\text{Na}^+$  complexation reduces the Stokes shift. In analogy to the well-known planarization of the excited state of biphenyl,<sup>11</sup> we believe that in the excited state the uncomplexed bithiophenes relax to a planarized state. The reorganization prior to the radiative decay also produces a change in the charge distribution. Reorganization produces a more polar excited state as the emission of the polymer **2** (without  $\text{Na}^+$ ) is blue shifted by 14 nm when the solvent is changed from THF to the much less polar hexane. The UV-vis was insensitive to solvent polarity, suggesting that the initial  $S_1$  state is less polar than the reorganized  $S_1'$  state. Due to the extreme insolubility of  $\text{NaClO}_4$  in hexane we were unable to perform the same experiment in the presence of  $\text{Na}^+$ .

The fact that the addition of  $\text{Na}^+$  reduces the lifetimes of both **2** and **3** lends additional support to the proposed mode of

action of  $\text{Na}^+$  on **2** and **3**. The geometry of the ground state ( $S_0$ ) more closely resembles the unrelaxed excited state ( $S_1$ ) rather than the relaxed excited state ( $S_1'$ ). Thus the rate of the  $S_1 \rightarrow S_0$  transition is greater than the rate of the  $S_1' \rightarrow S_0$  transition. Consequently, and in accordance with our observations, the  $\text{Na}^+$  complexed system is expected to have a shorter lifetime than the uncomplexed system.

Compound **3** has two physical states, complexed and uncomplexed, as evidenced by the presence of a clean isosbestic point in the UV-vis spectrum and a clean isoemissive point in the emission spectrum. In this case, the molecules containing complexed conformationally locked receptors are in equilibrium with molecules containing uncomplexed receptors which are able to reorganize in the excited state. The result is a nearly linear change in the wavelength of emission upon the addition of  $\text{Na}^+$ .

In the case of the polymer system, it should be noted that **2-H** and **2-M** behave differently than **2-L**. This appears to suggest that the effective length of the conjugation in these systems is greater than 2 repeat units but less than or equal to 4 repeat units. This is consistent with the effective conjugation length of polythiophene which is about 7 repeat units.<sup>12</sup> Thus the spectral characteristics of receptor units that are more than three to four repeat units removed from the site of complexation are essentially unaffected.

Consider the simpler case of the short polymer **2-L** where the average degree of polymerization is about 2 (see Figure 7). At lower concentrations of  $\text{Na}^+$ ,  $\text{Na}^+$ -bound sites will be flanked by at least one uncomplexed site. In accordance with the well-known phenomenon of energy migration in conjugated systems,<sup>5</sup>

(11) See pp 7 and 8 in: Lakowicz, J. R. *Principles of Fluorescence Spectroscopy*, Plenum Press: New York, 1986.

(12) Thienpont, H.; Rikken, G. L. J. A.; Meijer, E. W.; Hoeve, W. T.; Wynberg, H. *Phys. Rev. Lett.* **1990**, *65*, 2141.

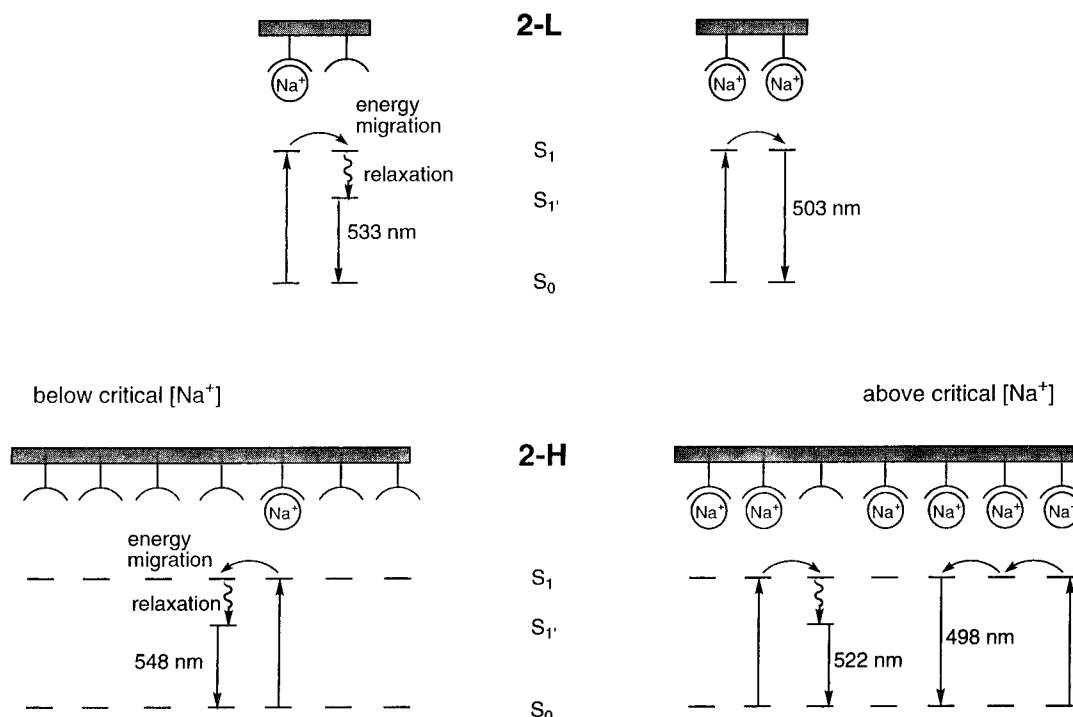


**Figure 7.** Schematic representation of **2-L** (top) and **2-H** (bottom) below (left) and above (right) the critical [Na<sup>+</sup>]. Below the critical [Na<sup>+</sup>], the excitation can migrate to an unoccupied site, relax, and emit a photon at the longer wavelength (548 nm). Above the critical [Na<sup>+</sup>] in the longer polymer chains (**2-H**), there are a few unoccupied sites flanked by Na<sup>+</sup>-bound sites. These unoccupied sites give rise to the shoulder at 522 nm (see Figure 3). The bulk of the emission (at 498 nm) arises from the bound sites.

the excitation can potentially migrate from the complexed receptor to a neighboring uncomplexed receptor that undergoes relaxation (planarization in this case) and emits light at the longer wavelength. As the concentration of Na<sup>+</sup> increases, the chains start to become saturated with Na<sup>+</sup> and it is no longer possible for the excitation to migrate and relax. Thus the emission shifts to a shorter wavelength.

Note that the above explanation does not preclude the possibility that the observed behavior arises due to a simple two-state system. To try and answer this question, we decided to do some simple modeling experiments. The initial emission curve (obtained before any NaClO<sub>4</sub> was added) was assumed to be the emission of the unbound species only. The final emission curve was assumed to arise solely from the Na<sup>+</sup>-bound species. If the observed behavior were indeed due to a two-state system, then the intermediate curves would be a weighted average of the curves due to the bound and unbound species. The simulated set of emission curves closely matched the observed emission curves for the model **3**. However, in the case for the polymer **2** simulations were quite different.

As mentioned earlier, the effective conjugation length is about 3 or 4 repeat units. Thus the chromophore in **2-L** is shorter than the effective conjugation length whereas the reverse is true for **2-H** and (to a lesser extent) for **2-M**. We now consider the case of **2-M** and **2-H** (see Figure 7). At [Na<sup>+</sup>] below the critical concentration, energy migration along the conjugated backbone from the complexed sites to uncomplexed ones takes place and thus there is little change in the emission. As the critical concentration is reached, more and more of the sites are occupied by Na<sup>+</sup> and the excitation can no longer find an uncomplexed site. The emission now takes place from the unrelaxed excited state, thus shifting to a shorter wavelength. In addition it is possible, considering electrostatic effects, that at no point (even in the presence of a gross excess of Na<sup>+</sup>) are all of the receptor sites on the chain occupied. We now have

the case where the polymer consists of segments of Na<sup>+</sup>-bound sites interrupted by one or more empty sites. The emission from these unbound sites which are flanked by Na<sup>+</sup>-bound sites may be the source of the shoulder on the low energy side of  $\lambda_{\max}$  (at  $\sim 520$  nm, see Figure 7). Since **2-H** has a longer chain length, the shoulder is more pronounced than is the case for **2-M**.

## Conclusion

We have prepared a conjugated polymer that can serve as a sensor that is selective for Na<sup>+</sup> over Li<sup>+</sup>, K<sup>+</sup>, and Ca<sup>2+</sup>. Binding of the Na<sup>+</sup> ion leads to only minor changes in the absorption spectra of both **2** and **3**. In contrast, Na<sup>+</sup> binding has a significant effect on the emission spectra of both **2** and **3**. This effect is more pronounced for the polymeric system **2**. The changes in the emission spectrum probably arise due to two factors: (1) conformational constraints introduced in the receptor unit due to Na<sup>+</sup> binding and (2) energy migration. Our future efforts in these types of systems will focus on the use of energy migration processes to generate a digital chemosensory response.

## Experimental Section

**General Methods.** UV-vis absorption measurements were performed on a Perkin-Elmer Lambda 9 UV/VIS/NIR spectrophotometer at 1 nm resolution. Fluorescence measurements were performed on a SPEX Fluorolog 3-12 Tau at 1 nm resolution. The instrument was equipped with a Xenon arc lamp and a Motor Driver that also allows for magnetic stirring of solutions in the sample holder itself.

Lifetimes were measured by using a SPEX Fluorolog 3-12 Tau fluorimeter with a Xenon lamp and a Pockels cell for varying the intensity of the exciting radiation. A colloidal suspension of glycogen in water (a scatterer;  $t = 0$ ) was used as the reference. For **2** measurements were made at 15.0, 19.5, 25.4, 33.0, 42.9, 55.8, 72.6, 94.4, 122.7, 159.6, 207.6, and 270 MHz. For **3** measurements were made at 50.0, 58.8, 69.3, 81.5, 95.9, 112.9, 132.9, 156.4, 184.0, 216.6, and 254.9 MHz.

Measurements were performed in  $5.0 \times 10^{-6}$  M THF solutions (based on the repeat unit molecular weight for the polymer) for both **2** and **3** and in  $2.4 \times 10^{-5}$  M THF solutions for **2-H**, **2-M**, and **2-L**. For a given set of measurements, excluding the polymer– $\text{Na}^+$  measurements, a set of 8 vials was arranged and 3 mL of solution of **2** or **3** was added to each. To the vials were then added aliquots of salt solution ( $\text{LiClO}_4$  (0.16 M in acetonitrile);  $\text{NaClO}_4$  (0.20 M in acetonitrile); or  $\text{KPF}_6$  (0.16 M in acetonitrile)) so as to create the concentration gradient described above (see text). After allowing the solutions to stand/equilibrate for 1 to 2 h the UV–vis spectrum of each solution was measured. That solution was then transferred to a 4-wall luminescence cuvette and its fluorescence measured. This procedure was repeated for all 8 solutions. Alternately, in the case of the polymer  $\text{Na}^+$  emission measurements, the fluorescence 4-wall cuvette was charged with 3 mL of polymer solution and a magnetic stir bar. Aliquots of salt solution were added at the prescribed increments. Solutions were allowed to equilibrate for at least 10 min before taking the measurement. Experimentation with longer equilibration times did not produce noticeable differences. This second method appeared to produce cleaner results.

Quantum yield measurements were made with quinine sulfate as reference. Solutions were excited at 365 nm and a quantum yield of 0.546 was assumed for the reference. All emission spectra obtained for quantum yield measurements were corrected to account for variances in detector response.

Polymer fractionation was done on a HP Series 1100 HPLC/GPC equipped with a diode array detector and with a HP PLGel 5  $\mu\text{m}$  column. The eluent was THF at a flow rate of 1 mL/min. After the solvent was evaporated, the residue was washed repeatedly with HPLC grade methanol to remove BHT stabilizer.

#### Calculation of the Stability Constant of the Complex between **3** and $\text{Na}^+$ According to the Method of Benesi and Hildebrand.<sup>8</sup> (**1**)

**From UV–vis data:** At 315 and 415 nm a plot of  $1/\epsilon$  versus  $1/[\text{Na}^+]$  was fitted to a straight line ( $y = mx + c$ ). Stability constant =  $y$ -intercept/slope =  $c/m$ . At 315 nm,  $1/\epsilon = 1.09 \times 10^{-7}/[\text{Na}^+] + 1.18 \times 10^{-4}$  ( $R^2 = 0.9989$ ). This leads to a binding constant  $K = 1.1 \times 10^3 \text{ M}^{-1}$ . At 415 nm,  $1/\epsilon = 1.21 \times 10^{-7}/[\text{Na}^+] + 2.04 \times 10^{-4}$  ( $R^2 = 0.9963$ ). This leads to a binding constant  $K = 1.7 \times 10^3 \text{ M}^{-1}$ .

(2) **From emission data:** At 425, 475, and 500 nm a plot of  $1/(\text{emission intensity})$  versus  $1/[\text{Na}^+]$  was fitted to a straight line ( $y = mx + c$ ). Stability constant =  $y$ -intercept/slope =  $c/m$ . At 425 nm,  $1/(\text{emission intensity}) = 8.51 \times 10^{-11}/[\text{Na}^+] + 1.84 \times 10^{-7}$  ( $R^2 = 0.9933$ ). This leads to a binding constant  $K = 2.2 \times 10^3 \text{ M}^{-1}$ . At 475 nm,  $1/(\text{emission intensity}) = 1.21 \times 10^{-10}/[\text{Na}^+] + 2.79 \times 10^{-7}$  ( $R^2 = 0.9936$ ). This leads to a binding constant  $K = 2.3 \times 10^3 \text{ M}^{-1}$ . At 500 nm,  $1/(\text{emission intensity}) = 9.64 \times 10^{-11}/[\text{Na}^+] + 1.96 \times 10^{-7}$  ( $R^2 = 0.9931$ ). This leads to a binding constant  $K = 2.0 \times 10^3 \text{ M}^{-1}$ . The average of these five values gives  $K = 1.9 \times 10^3 \text{ M}^{-1}$ .

**Synthesis.** The synthesis of the calixarene diiodide **1** (Scheme 1) has been reported previously (see ref 6).

**Model System 3.** A mixture of **1** (60 mg, 0.051 mmol), 2,5-dimethoxyphenylboronic acid (57 mg, 0.31 mmol, 6 equiv), triphenylphosphine (20 mg, 0.076 mmol),  $\text{Pd}(\text{dba})_2$  (2 mg, 0.0035 mmol, 7 mol %), and  $\text{Ti}_2\text{CO}_3$  (0.77 g, 1.6 mmol) in a 25 mL Schlenk flask was

evacuated and back-filled with Ar three times. The mixture was treated with THF (5 mL) and water (1 mL) and purged with Ar for about 20 min before being heated to 70 °C for 16 h. The mixture was cooled and filtered through silica gel with ether. The filtrate was evaporated under reduced pressure to give 75 mg of brown solid. Silica gel chromatography (80% hexane, 20% ethyl acetate) gave **3** (49 mg, 82%).  $^1\text{H}$  NMR (250 MHz,  $\text{CDCl}_3$ ):  $\delta$  0.82 (s), 0.95 (s), 1.00 (s), 1.22 (s), 1.26 (s), 1.29 (s), 1.34 (s), 3.1–3.3 (m), 3.37 (s), 3.57 (s), 3.78 (s), 3.83 (s), 4.36 (d), 4.48 (m), 4.75 (t), 6.49 (s), 6.71 (s), 6.80 (dd), 6.92 (d), 7.08 (m), 7.15 (d), 7.19 (m), 7.24 (s), 7.33 (s), and 7.41 (s).  $^{13}\text{C}$  NMR (62.9 MHz,  $\text{CDCl}_3$ ):  $\delta$  31.07, 31.61, 37.93, 55.80, 56.30, 62.05, 72.08, 73.11, 73.17, 119 (2), 123, 124.53, 126, 126.09, 131.79, 132, 133.31, 135.19, 135.70, 126, 137, 143–146 (5), 150, 154, and 155. HRMS (FAB): found,  $m/z$  1199.5694 ( $\text{M} + \text{H}^+$ ); calcd for  $\text{C}_{74}\text{H}_{86}\text{O}_{10}\text{S}_2$   $m/z$  1198.5662.

**Polymer 2.** A 25 mL Schlenk flask was charged with **1** (91.8 mg, 0.078 mmol, 1 equiv), 2,5-didecyloxyphenyl-1,4-diboric acid (38.4 mg, 0.079 mmol, 1 equiv),  $\text{Pd}(\text{dba})_2$  (0.5 mg, 0.0009 mmol, 1 mol %), triphenylphosphine (20 mg, 0.076 mmol), and  $\text{Ti}_2\text{CO}_3$  (0.64 gm, 1.4 mmol), evacuated, and back-filled with Ar three times. To this mixture were added THF (5 mL) and water (1 mL); the mixture was purged with Ar for 30 min and heated to 75 °C for 60 h. The mixture was then cooled, diluted with ethyl acetate (125 mL), filtered, and evaporated to give a brown solid. The polymer was purified by dissolving in  $\text{CHCl}_3$  and precipitating from MeOH three times. Polymer **2** was isolated as an orange solid (50 mg, 50%) with  $M_n = 4500$  g/mol relative to PS standards ( $\text{PDI} = 1.55$ ).  $^1\text{H}$  NMR (250 MHz,  $\text{CDCl}_3$ ):  $\delta$  0.84 (m), 0.95 (s), 1.1–1.7 (m), 1.94 (br), 3.12–3.38 (m), 3.58 (s), 3.89–4.15 (br m), 4.33–4.49 (br m), 4.76 (br), 6.49 (s), 6.71 (br s), 6.85 (br d), 7.05–7.24 (br m), and 7.35–7.49 (br m).  $^{13}\text{C}$  NMR (62.9 MHz,  $\text{CDCl}_3$ ):  $\delta$  14.12, 22.67, 26.09, 26.37, 29.33, 29.60, 30.58, 31.09, 31.27, 31.63, 31.89, 33.59, 33.76, 34.10, 37.98, 58.09, 62.09, 68.71, 69.67, 72.16, 72.92, 73.25, 111.53, 113.57, 113.86, 119.20, 122.62, 124.58, 125.19, 125.51, 126.11, 126.46, 131.79, 131.99, 133.33, 135.20, 135.03, 136.58, 144.34, 144.56, 144.87, 145.20, 145.98, 149.61, 153.16, 153.95, 154.48, 154.99, and 155.29.

**Acknowledgment.** The authors wish to acknowledge Dr. Jye-Shane Yang for providing significant insights into fluorescence spectroscopy, for fruitful discussions, and for assistance with many practical aspects of fluorescence spectroscopy. We thank Prof. Michael Sponsler for his valuable suggestions. We also acknowledge Dr. Igor Levitsky for assistance with the lifetime measurements. We are grateful for financial support from the Office of Naval Research and DuPont. This work was also supported by a Camille Dreyfus Teacher-Scholar Award and Alfred P. Sloan Research Fellowship to T.M.S.

**Supporting Information Available:** Details of the simulations for the emission of **2** and **3** in the presence of  $\text{Na}^+$  (5 pages, print/PDF). See any current masthead page for ordering information and Web access instructions.

JA9737230